Study of the solid-state 'amorphization' reaction in $Fe_{50}Re_{50}$ by means of Mössbauer spectrometry and diffraction measurements

2002 J. Phys.: Condens. Matter 14 9713

(http://iopscience.iop.org/0953-8984/14/41/326)

INSTITUTE OF PHYSICS PUBLISHING JOURNAL OF PHYSICS: CONDENSED MATTER

J. Phys.: Condens. Matter **14** (2002) 9713–9724 PII: S0953-8984(02)52088-9

Study of the solid-state 'amorphization' reaction in $Fe_{50}Re_{50}$ by means of Mössbauer spectrometry and diffraction measurements

N Randrianantoandro[1], R J Cooper[2], J-M Greneche[1] and N Cowlam[1,2]

[1] Laboratoire de Physique de l'Etat Condensé, UMR CNRS 6807, Université du Maine, 72085 Le Mans Cedex 9, France
[2] Department of Physics and Astronomy, University of Sheffield, Sheffield S3 7RH, UK

Received 7 August 2002
Published 4 October 2002
Online at stacks.iop.org/JPhysCM/14/9713

Abstract

The solid-state 'amorphization' reaction produced by the mechanical alloying (MA) of the equiatomic alloy $Fe_{50}Re_{50}$ has been studied using ^{57}Fe Mössbauer spectrometry plus x-ray and neutron diffraction. The percentages of iron atoms in the magnetic phases present in the reaction have been obtained from the Mössbauer spectra and the consumption of the parent elements derived from the reduction in intensity of their Bragg peaks in the diffraction patterns. The reaction in the $Fe_{50}Re_{50}$ alloy appears to be 2–3 times slower than the reaction in the related $Fe_{58}Ta_{42}$ alloy studied by us previously. A possible reason for this is the presence of an intermediate phase in the reaction revealed by the hyperfine structure at ^{57}Fe. This is identified as an iron-rich solid solution by the absence of any new Bragg peaks in the diffraction patterns. Although a small fraction of the rhenium remains unconsumed at the end of the reaction, the FeRe alloy obtained after 24 h of MA has a genuine amorphous structure, whose reduced radial distribution function $G(r)$ is sensitive to the topological order present.

1. Introduction

Transition metal–refractory metal (TM–RM) alloys are known to glass form over a narrow composition range close to the equiatomic value [1–3], but they can be difficult to prepare by chill-block melt-spinning on account of their high melting points. They are, however, accessible by solid-state 'amorphization' reactions so we have made a systematic investigation of the formation and properties of TM–RM amorphous alloys produced by mechanical alloying (MA) [4]. Indeed most of these binary systems exhibit positive Gibbs energy of formation as has been discussed earlier in the case of the Fe–W system [5]. Preliminary results on amorphous $Fe_{58}Ta_{42}$ alloys have already been presented [6, 7]. The percentages of iron atoms in the magnetic phases present can be determined for the iron-based TM–RM alloys

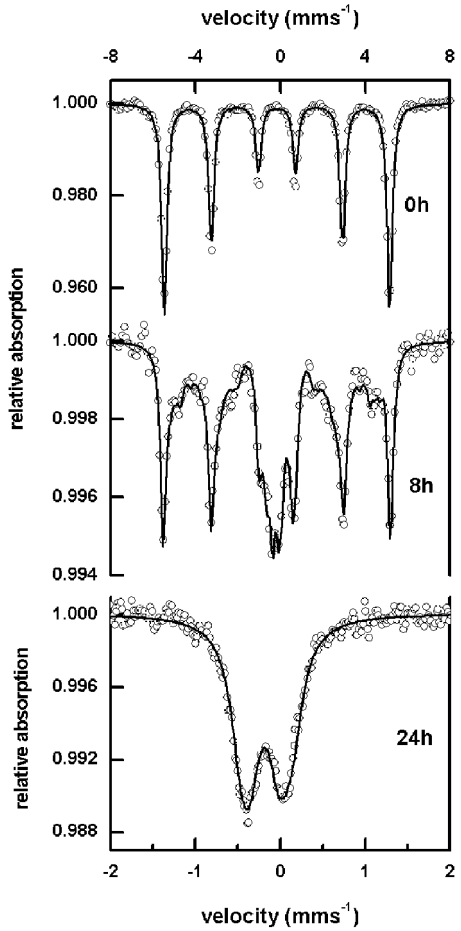

Figure 1. Three characteristic Mössbauer spectra for the $Fe_{50}Re_{50}$ alloys with $t = 0$, 8, 24 h and measured at 300 K, are shown. Note the change of scale of the source velocity.

by Mössbauer spectrometry. Neutron diffraction can also provide an accurate measurement of the consumption of the *transition metal* in both Fe–RM and Ni–RM alloys because iron and nickel have large values of nuclear scattering length. In addition, x-ray diffraction gives an accurate measurement of the consumption of the heavier *refractory metal*. The reaction in the Fe–RM alloys can therefore be investigated using Mössbauer spectrometry and diffraction with a precision that cannot always be achieved for other alloy systems. The reaction in the equiatomic $Fe_{50}Re_{50}$ alloy will be described in the present paper, concentrating on the crystalline-to-amorphous transition at the atomic level and making some comparisons with $Fe_{58}Ta_{42}$ [6, 7]. A study of the changes in the large-scale structures of these samples, using small-angle neutron scattering (SANS), will be published elsewhere [8].

2. Sample preparation and experimental methods

Iron powder of 4N8 purity (Koch-Light) and rhenium powder of 3N purity (Aldrich) were mixed in the atomic concentration $Fe_{50}Re_{50}$. The initial series of samples had undergone MA treatments for $t = 0$ (parent), 2, 4, 8, 16 and 24 h; to this series, further specimens which had

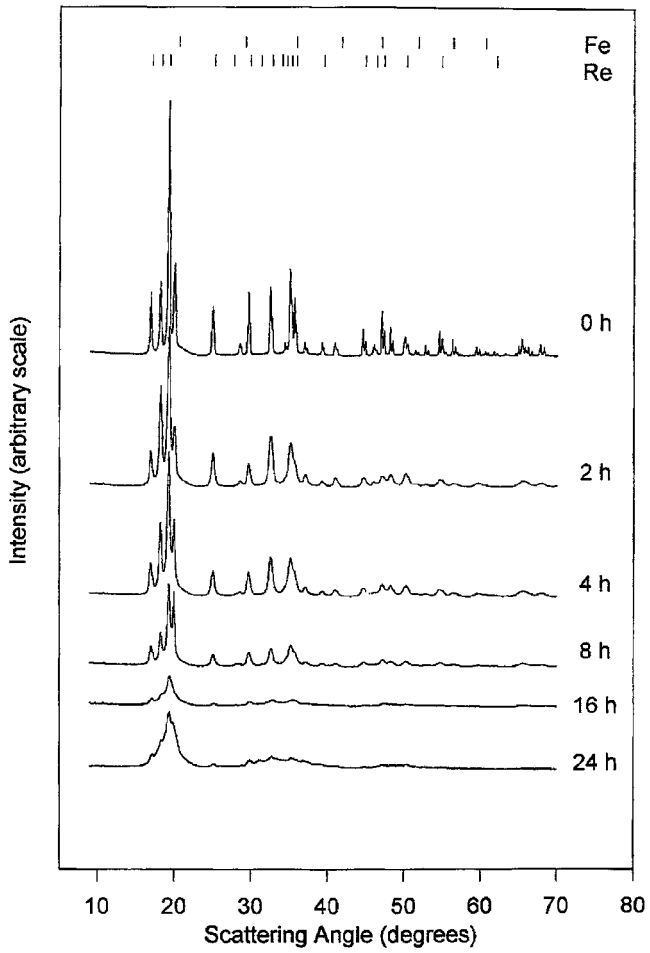

Figure 2. The x-ray diffraction patterns for the $Fe_{50}Re_{50}$ alloys MA treated for $t = 0$, 2, 4, 8, 16 and 24 h are shown.

undergone MA for $t = 10$, 12 were added later for the Mössbauer measurements. A SPEX 8000 mixer/mill (which has a fixed intensity of milling) was used with a tool steel vial, two 12 mm steel balls and a standard charge of 6 g of powder. The MA was performed under argon to prevent oxidation. Because of the rather short milling times, no significant contamination occured, unlike the case of the Fe–W system treated using a planetary mill (Fritsch Pulverisette P5) [5].

The ^{57}Fe Mössbauer experiments were performed in transmission geometry, at 300 and 77 K, using a constant-acceleration signal spectrometer with a ^{57}Co source dispersed into a rhodium matrix. The samples each consisted of a mixture of the $Fe_{50}Re_{50}$ and boron nitride (BN) powders enclosed in a thin polymer capsule of diameter 20 mm. The data acquisition time for each Mössbauer spectrum was 48 h, on account of the large absorption cross-section for γ-rays of the rhenium atoms.

Examples of three of the spectra measured at 300 K are shown in figure 1, with a change of energy range between the samples with times of MA treatment $t = 8$ and 24 h. The familiar magnetic sextet of ferromagnetic α-Fe can be recognized in the spectrum of the parent sample. It progressively collapses to a quadrupolar doublet for samples with longer times of MA when the amorphous phase is fully established. The hyperfine structures are rather

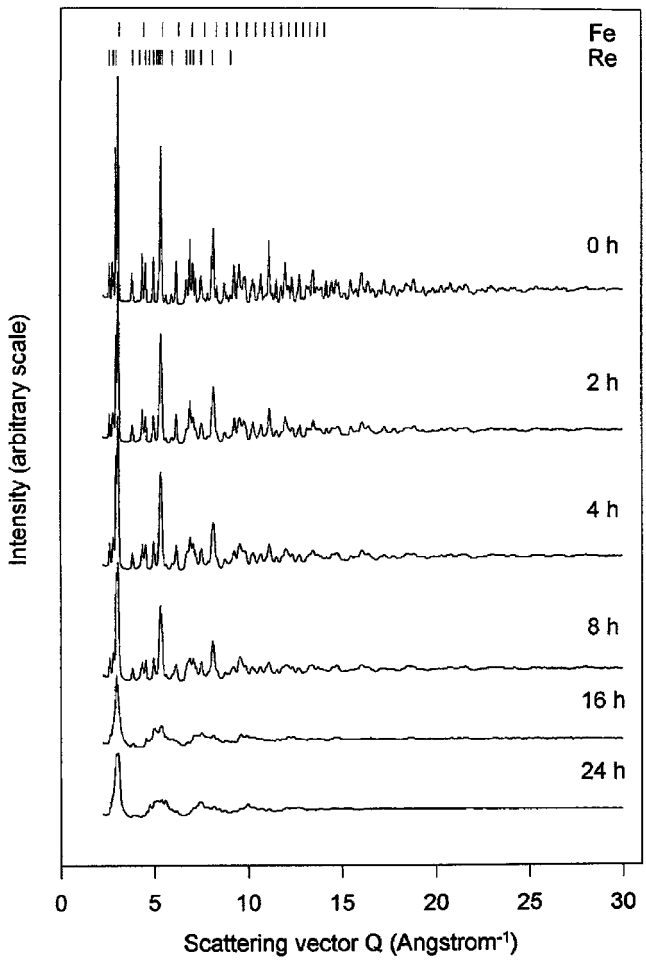

Figure 3. The neutron diffraction patterns for the $Fe_{50}Re_{50}$ alloys with $t = 0$, 2, 4, 8, 16 and 24 h, from the LAD instrument at ISIS, are shown.

complex for samples treated for intermediate times such as the $t = 8$ h sample, which contains more than two components which will be discussed in detail below. Figure 1 shows that the solid-state reaction in the equiatomic $Fe_{50}Re_{50}$ alloy is clearly much slower than that in $Fe_{50}Ta_{50}$ [6, 7] even though the same SPEX 8000 mill was used under identical conditions in the two investigations. Comparing figure 1 with figure 3 of [6], shows that the quadrupolar doublet is already established in the Mössbauer spectrum of the $Fe_{58}Ta_{42}$ alloy after just $t = 3$ h, whereas a similar spectrum is not observed for the $Fe_{50}Re_{50}$ alloy until after $t = 8$ h.

The x-ray diffraction experiments were carried out with a Philips PW1050 vertical diffractometer, a graphite monochromator and Mo Kα radiation ($\lambda = 0.711$ Å). The samples were measured in a conventional flat-plate holder. The x-ray diffraction patterns are shown in figure 2, for scattering angles in the range $7° < 2\theta < 70°$. Those for the samples with $t < 8$ h exhibit well-defined Bragg peaks from the bcc iron and the hcp rhenium, which are identified at the top of the figure. The first three intense peaks are from rhenium, which scatters about seven times more strongly than the iron. The Bragg peaks broaden and reduce in intensity with increasing time t of MA treatment. The patterns for samples with $t > 16$ h show the diffuse

scattering of the amorphous FeRe phase; superimposed upon these, weak Bragg peaks from a small fraction of unconsumed rhenium can be seen. It is not normally possible to reduce this fraction by just changing the starting composition, since the driving force for the reaction is also dependent on the composition. Again comparing figure 2 with figure 1 of [6] shows that the diffuse scattering pattern of the amorphous phase is established after $t = 6$ h for the $Fe_{58}Ta_{42}$ alloy, but not until $t = 16$ h for the $Fe_{50}Re_{50}$.

The neutron diffraction measurements were carried out on the LAD instrument (time-of-flight mode) at the ISIS, RAL, Chilton. The specimens were examined in thin-walled vanadium tubes and the necessary background and normalization scans were also performed. The neutron diffraction patterns are shown in figure 3 for values of the scattering vector $2.5\ \text{Å}^{-1} < Q < 30\ \text{Å}^{-1}$. Since iron and rhenium have similar values of the nuclear scattering length ($b_{\text{Fe}} = 0.954 \times 10^{-12}$ cm and $b_{\text{Re}} = 0.92 \times 10^{-12}$ cm), their contributions to the patterns are effectively equal, although the most intense peaks are from the bcc iron. The reduction in intensity and the broadening of the Bragg peaks with increasing time t are particularly evident in the range $10\ \text{Å}^{-1} < Q < 20\ \text{Å}^{-1}$. The transition from the crystalline to the amorphous state beyond $t = 16$ h is also clear and confirms the increase in the reaction time for $Fe_{50}Re_{50}$ compared with $Fe_{58}Ta_{42}$ which has already been referred to.

3. Data analysis

3.1. Mössbauer spectrometry

The Mössbauer spectra were analysed by the method used previously to study the $Fe_{52}Ta_{48}$ alloys [6]. A least-squares refinement was made to fit each spectrum with:

(a) a magnetic sextet (of the parent α-Fe) and
(b) an asymmetric quadrupolar doublet (of the amorphous FeRe alloy), both based on Lorentzian lineshapes.

The two components (i) and (ii) can be identified in figure 1. However, the spectral lines of the sextet broaden and decrease in intensity in the early stages of the reaction and these spectra can be refined using a distribution of hyperfine fields. Figure 4 shows the distribution of hyperfine fields obtained from the spectra of the $t = 2, 4, 8$ and 10 h samples measured at 300 and 77 K. The main peak corresponds to the value for α-Fe ($B_f = 33$ T at 300 K and $B_f = 34$ T at 77 K) in each case, but as the time of MA increases, a broad distribution of hyperfine fields appears for values in the range $10\ \text{T} < B < 30\ \text{T}$. The magnetic sextet and the asymmetric quadrupolar doublet were subtracted numerically from the total spectra of these $t = 2, 4, 8$ and 10 h samples, in order to isolate this third contribution. The least-squares refinement of these spectra was therefore based on the presence of three components, namely:

(i) a sextet;
(ii) a second sextet with broadened spectral lines; and
(iii) an asymmetric quadrupolar doublet.

The results of this refinement are shown in figure 5 and the Mössbauer parameters of the constituent spectra are given in table 1. The values of the isomer shift (IS) are quoted relative to that of α-Fe at room temperature. We have explained previously [6] that the asymmetry of the doublet (iii) can be fitted most successfully with only two quadrupolar doublets with two weakly differing ISs as specified in table 1.

It is clear that contribution (i) above is unalloyed α-Fe and that (iii) is the paramagnetic, amorphous FeRe alloy produced in the reaction. The broadening of the spectral lines of the sextet is most probably caused by a change in the local environments of a fraction of the iron

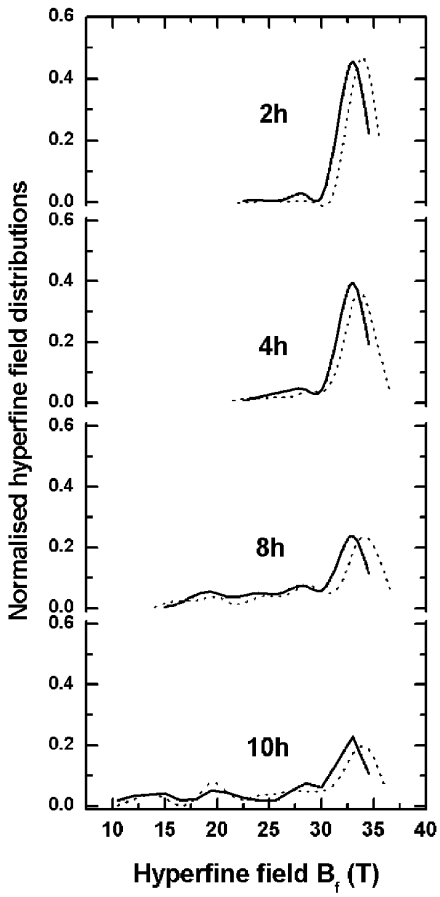

Figure 4. The hyperfine field distributions $P(B_f)$ versus B_f for the $Fe_{50}Re_{50}$ alloys with $t = 2$, 4, 8 and 10 h are shown, measured at 300 K (solid curve) and 77 K (dotted curve).

atoms in the sample. Table 1 shows that the hyperfine parameters of component (ii) have values (i.e. -0.15 mm s^{-1} < IS < 0.02 mm s^{-1} and 20 T < B < 29 T) which are similar to those for ferromagnetic iron-rich solid solutions found in the literature. In addition, figure 4 and table 1 show that the distribution of hyperfine fields shifts toward smaller values of B as the time of MA increases, which is consistent with a dilution of the first-neighbour iron atoms by the non-magnetic rhenium. We will therefore describe this (ii) component as an 'intermediate' phase with the indication that it may be a solid solution, possibly situated at the interfaces between the powder grains of iron and rhenium.

Providing that the three components (i)–(iii) all have the same value of the recoil-free fraction (f-factor), then the relative percentages of the iron atoms present in each of the phases in the sample are directly proportional to the area under their spectral peaks. Hence the consumption of the α-Fe can be obtained for comparison with the diffraction data as shown in figure 6(a). An indication of the corresponding growth of the two other phases in the reaction can be obtained from the percentage of iron atoms present, because there is no information on the rhenium concentration. Finally, it is important to emphasize that the results obtained from the series of spectra recorded at 77 K agree completely with those at 300 K, revealing no occurrence of magnetic fluctuations, i.e. superparamagnetic effects.

Table 1. The values of the hyperfine parameters and the relative percentages for the components in the Mössbauer spectra recorded at 300 K for the MA-treated $Fe_{50}Re_{50}$ alloys are given. IS is the isomer shift; Γ is the linewidth at half-height, QS is the quadrupolar splitting, 2ε is the quadrupolar shift and $\langle B_f \rangle$ is the hyperfine field.

MA time t (h)	Component of spectra	IS (mm s^{-1}) ±0.01	Γ (mm s^{-1}) ±0.01	2ε or QS (mm s^{-1}) ±0.01	$\langle B_f \rangle$ (T) ±0.5	Relative per cent of iron atoms (%) ±2
0	Magnetic sextet (α-Fe)	−0.00	0.30	0.00	32.8	100
2	Magnetic sextet (α-Fe)	−0.00	0.30	0.01	32.9	89
	Intermediate phase	0.02	0.30	0.27	28.1	8
	Quadrupolar doublet 1	−0.02	0.32	0.40	0	1
	Quadrupolar doublet 2	0.20	0.28	1.28	0	2
4	Magnetic sextet (α-Fe)	−0.00	0.30	0.00	33.0	74
	Intermediate phase	−0.10	0.30	−0.03	27.8	19
	Quadrupolar doublet 1	0.14	0.32	0.32	0	4
	Quadrupolar doublet 2	0.14	0.28	1.26	0	3
8	Magnetic sextet (α-Fe)	0.00	0.30	−0.02	33.0	38
	Intermediate phase	−0.07	0.30	−0.03	24.6	41
	Quadrupolar doublet 1	−0.01	0.32	0.30	0	14
	Quadrupolar doublet 2	0.14	0.28	1.15	0	7
10	Magnetic sextet (α-Fe)	0.00	0.36	−0.00	33.1	17
	Intermediate phase	−0.14	0.36	0.05	20.8	17
	Quadrupolar doublet 1	−0.05	0.36	0.38	0	54
	Quadrupolar doublet 2	0.03	0.28	0.94	0	12
12	Quadrupolar doublet 1	−0.05	0.32	0.34	0	76
	Quadrupolar doublet 2	−0.01	0.28	0.72	0	24
16	Quadrupolar doublet 1	−0.07	0.32	0.31	0	64
	Quadrupolar doublet 2	−0.03	0.28	0.69	0	36
24	Quadrupolar doublet 1	−0.05	0.32	0.36	0	68
	Quadrupolar doublet 2	−0.03	0.28	0.61	0	32
32	Quadrupolar doublet 1	−0.05	0.32	0.35	0	68
	Quadrupolar doublet 2	−0.03	0.28	0.66	0	32

3.2. X-ray and neutron diffraction

The diffraction patterns were initially analysed as before [6], and the intensities of the Bragg peaks of the iron and the rhenium were summed (to a given value of Q) and the sums normalized to the sample weight. These summed intensities $\sum I(t)$, for each different time t of MA treatment, were then normalized to the intensity $\sum I_0$ of the parent (0 h) sample. Graphs of $\sum I(t)/\sum I_0$ versus t are given in figure 6(b) for comparison with the Mössbauer data and also with the equivalent results for $Fe_{50}Ta_{50}$ shown in figure 4 of [6]. An attempt to describe the consumption of the constituents in the reaction by the usual exponential, $\frac{\sum I(t)}{\sum I_0} = \exp(\frac{-t}{\tau})$, was not very successful. In particular, the value of $\tau_{Fe} \approx 9$ h obtained from the diffraction patterns was inconsistent with the absence of Bragg peaks from iron in the diffraction patterns of the $t = 16$ and 24 h samples and especially the absence of a sextet contribution in the Mössbauer spectrum of the $t = 12$ h sample.

A simple exponential decrease of the Bragg peak intensities of the parent elements will not be observed if the 'intermediate' phase has the same structure type as one of the parents,

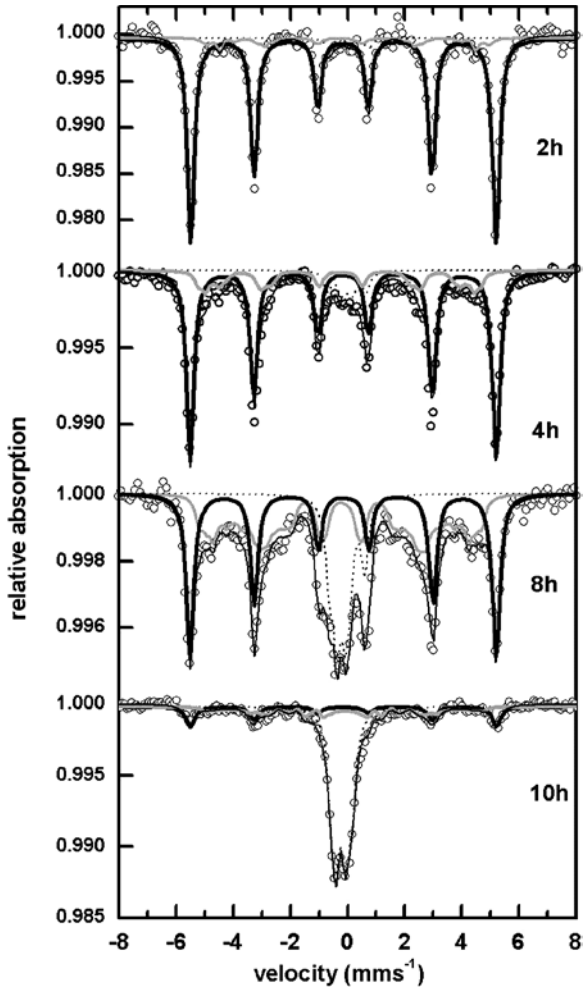

Figure 5. The Mössbauer spectra for the $Fe_{50}Re_{50}$ alloys with $t = 2$, 4, 8 and 10 h are shown decomposed into the contributions from the three phases (i)–(iii) described in the text. The measurements were made at 300 K. (i) ▬: α-Fe; (ii) ▬: intermediate phase; (iii) ▪▪▪▪▪: amorphous phase; ——: calculated spectrum; ○: experimental data.

such that their Bragg peaks overlap. The variation of their intensity with MA time will then be complex, rather like the growth of a radioactive daughter product in a radioactive decay series. The absence of any *new* Bragg peaks in the x-ray and neutron diffraction patterns suggests that the 'intermediate' phase is not an intermetallic compound. This is not therefore an example of the 'type III' solid-state reaction according to the classification proposed by Weeber and Bakker [9]. The favoured candidate for the 'intermediate' phase is an iron-rich α-Fe–Re solid solution, as will be discussed below.

4. The amorphous end-product

The reaction in the equiatomic $Fe_{50}Re_{50}$ alloy is therefore different from that in $Fe_{58}Ta_{42}$, which is 2–3 times faster and characterized by direct consumption of the parental elements

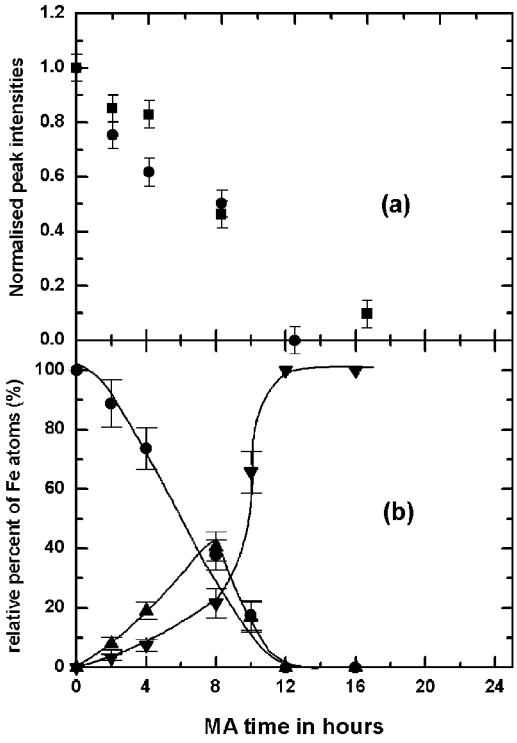

Figure 6. The evolution of the solid-state amorphization reaction in the MA $Fe_{50}Re_{50}$ alloys is shown. (a) Consumption of the parent phases from the diffraction data: iron (●) and rhenium (■). (b) Consumption of the α-Fe fraction (●) and the growth of the intermediate (▲) and amorphous phases (▼) from the Mössbauer data.

and a corresponding growth of the amorphous phase [6]. On the other hand, the values of the hyperfine parameters, e.g. the linewidth at half-height (Γ), the IS and the quadrupolar splitting (QS) given in table 1, for the fully transformed $Fe_{50}Re_{50}$ sample are very similar to those obtained for $Fe_{52}Ta_{48}$ [6]. This suggests that a similar kind of amorphous state has been produced, at least in terms of the local environments of the iron atoms.

This is also confirmed by the neutron diffraction pattern for the $t = 24$ h sample. It has a relatively sharp first peak and when the pattern is magnified, five further diffuse peaks can be identified out to $Q \approx 15$ Å^{-1}. These data were therefore normalized to obtain the total structure factor $S(Q)$ and the reduced radial distribution function $G(r)$ was derived by the normal Fourier transformation. The resulting curve shown in figure 7 has an excellent spatial resolution of $\Delta r = 0.21$ Å on account of the high value of Q_{max} accessible on the LAD instrument. The $G(r)$ has a first-neighbour peak at $r_1 = 2.68$ Å and the second peak, with its characteristic shoulder, is at $r_2 \approx 4.5$ Å. The nuclear scattering lengths of iron and rhenium are very similar, so the reduced RDF is related to the pair correlation functions by a symmetrical equation:

$$G(r) = 0.259G_{\mathrm{FeFe}}(r) + 0.500G_{\mathrm{FeRe}}(r) + 0.241G_{\mathrm{ReRe}}(r).$$

The *weighted* mean value of the first-neighbour distance obtained from the Goldschmidt radii of the constituents ($r_{\mathrm{Fe}} = 1.27$ Å and $r_{\mathrm{Re}} = 1.37$ Å) is $r_1 = 2.64$ Å, which is in good agreement with the observed distance. To emphasize that no information can be gained

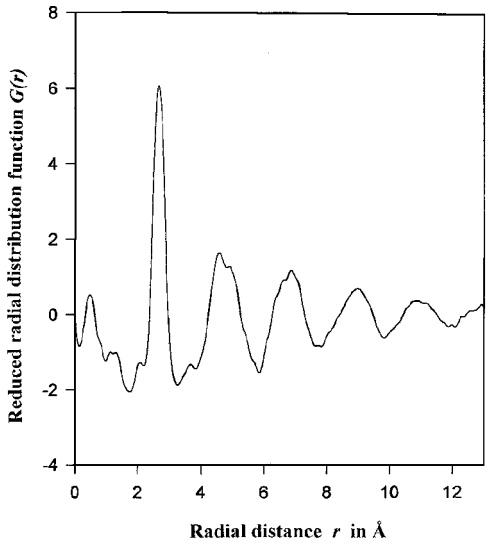

Figure 7. The reduced radial distribution $G(r)$ derived from the neutron diffraction pattern of the fully transformed $Fe_{50}Re_{50}$ alloy $t = 24$ h is shown.

about the atomic pair correlations within the first peak (even if they were not random), the Bhatia–Thornton [10] representation of the total structure factor gives

$$S(Q) \equiv 1.000 S_{NN}(Q)$$

to three decimal places. This confirms that the neutron data contain information about the topological structure alone.

5. Discussion and conclusions

The data presented in figure 6 allow the kinetics of the solid-state reaction in $Fe_{50}Re_{50}$ to be followed. The Mössbauer data show that the percentage of iron atoms located in the parental α-Fe falls regularly for times of MA in the range 0 h $< t <$ 8 h, so after $t >$ 12 h, the iron atoms are all in a paramagnetic state at room temperature. The growth of the FeRe amorphous alloy is initially slow, but the reaction appears to be complete and this phase fully established within a similar period $t \approx$ 12 h. The 'intermediate' phase is present in the samples which have undergone $t = 2, 4, 8$ and 10 h of MA and the fraction of iron atoms in this phase reaches $\approx$41% at $t = 8$ h but afterwards reduces. No new Bragg peaks are observed in the x-ray and neutron diffraction patterns, as verified by the flat background levels for $7^\circ < 2\theta < 30^\circ$ in figure 2 and for 2.5 Å$^{-1} < Q <$ 5.0 Å^{-1} in figure 3. The 'intermediate' phase must therefore be related to one of the phases that is already present in the sample, either an iron-rich solid solution, a rhenium-rich solid solution or a second amorphous phase.

A rhenium-rich solid solution is only a candidate in so far as figures 2 and 3 show the persistent, small fraction of unconsumed rhenium for the longer times of MA treatment. Such a phase is unlikely to be ferromagnetic or exhibit a broadened-sextet Mössbauer spectrum. This is also true of a second amorphous phase. It would, of course, be difficult to obtain information on the *growth* of such an amorphous phase from the diffraction data, because the *background* scattering level in the diffraction patterns becomes lost. Absolute rather than relative intensity measurements are required for volumetric measurements on amorphous materials. The fact that

component (ii) in the Mössbauer spectrum is a broad-line magnetic sextet strongly suggests that the 'intermediate' phase must be an iron-rich solid solution such as Fe_xRe_{1-x} with $x \geqslant 0.75$.

This identification agrees with our qualitative description of this reaction, in which the milling of the powder grains produces a lamellar composite with highly convoluted (fractal) interfaces [6], whose dimensions gradually reduce toward the characteristic diffusion lengths at the milling temperature. On the atomic level, fast diffusion occurs, here of the smaller iron atoms into the lattice of the larger rhenium atoms. Both interstitial and substitutional diffusion will occur, to accommodate the large mass transport, and the resulting (positive and negative) strain fields may help the crystalline-to-amorphous transition [11]. The intermediate phase is most probably an iron-rich α-Fe–Re solid solution created by the 'backwards' flux of rhenium atoms across the Fe:Re interfaces. The 'forward' flux of fast-diffusing iron atoms will eventually produce an alloy of $Fe_{50}Re_{50}$ composition by the *end* of the reaction, so the Re–Fe solid solution formed in the early stages is unlikely to be ferromagnetic. In addition, the flux of the heavier rhenium atoms into the iron lattice will enhance the *visibility* of the combined α-Fe and α-Fe–Re phases in the x-ray diffraction patterns. This will incidentally also complicate the application of a model involving the simple exponential consumption of parent α-Fe to the diffraction data.

The hyperfine field distributions given in figure 5 remain roughly the same shape when the temperature is reduced from 300 to 77 K, supporting our identification of the α-Fe–Re solid solution. The main peak does not broaden, but shifts towards the value for α-Fe at 77 K. These distributions are very similar to those observed in FeCr and FeW MA samples by Le Caer and colleagues [12] (see particularly figures 5, 7 and 8 of [13]). These authors have already suggested that these components may originate from the irregular interfaces between nanometre-size iron-rich regions and chromium- or tungsten-rich regions.

A more quantitative model of the reaction can be derived from the data in figure 6. The consumption of iron is indicated by the Mössbauer and diffraction data and the consumption of rhenium by just the diffraction data. This consumption indicates the fraction of atoms available at any time t to form the amorphous and 'intermediate' phases. We will postulate that the amorphous phase forms at the composition $Fe_{51}Re_{49}$ (on account of the small fraction of unconsumed rhenium), so the iron-rich α-Fe–Re 'intermediate phase' is likely to have an *average* composition halfway between this and the end-product, say $\approx Fe_{80}Re_{20}$. The Mössbauer data in figure 6(b) show the fraction of *the iron atoms* in both the amorphous and 'intermediate' phases, from which the fraction *of both* iron and rhenium atoms can be deduced by adopting the alloy compositions suggested above. The atomic fractions obtained in this way are given in table 2 and their smooth variation with t helps to confirm the validity of this model of the reaction. These values have not been plotted, since this information in table 2 is essentially complementary to that already presented in figure 6.

In conclusion, the solid-state reaction in the equiatomic $Fe_{50}Re_{50}$ alloy has been found to be 2–3 times slower than the equivalent reaction in $Fe_{58}Ta_{42}$. The Mössbauer data show clearly the presence of an 'intermediate' phase in the reaction of $Fe_{50}Re_{50}$ which can be identified with an iron-rich solid solution that is absent from $Fe_{58}Ta_{42}$. This 'intermediate' phase is most probably located at the highly convoluted fractal interfaces between the powder grains that have been observed by means of neutron small-angle scattering [7, 14]. A reaction in which the parental elements transform directly to the amorphous phase should proceed more quickly than one in which the interfaces are decorated by an intermediate phase. The free volume will always be greater in the amorphous product and this will enhance the fast diffusion across the interfaces, which is known to be a key feature of solid-state reactions.

Table 2. The atomic fractions of the phases present in the $Fe_{51}Re_{49}$ reaction are given as derived from the consumption of iron and rhenium from the Mössbauer and diffraction data and the growth of the amorphous and 'intermediate' phases from just the Mössbauer data. The amorphous and 'intermediate' phases are assumed in this model to have the compositions $Fe_{51}Re_{49}$ and $Fe_{80}Re_{20}$ respectively.

MA time	Atomic per cent of each phase present			
t (h)	α-Fe	Re	a-$Fe_{51}Re_{49}$	'Intermediate'
0	0.50	0.50	0	0
2	0.41	0.45	0.09	0.06
4	0.35	0.41	0.15	0.11
8	0.20	0.31	0.31	0.19
10	0.10	0.16	0.65	0.09
16	0	0.03	0.975	0
24	0	0.01	0.99	0

Acknowledgments

The neutron experiments were made within the EPSRC Neutron Beam Programme and the help of the staff at ISIS source is gratefully acknowledged. RJC held an EPSRC studentship during the course of this work. NC would like to acknowledge the hospitality of the UFR Sciences et Techniques, Université du Maine, and NR the hospitality of the Department of Physics and Astronomy, University of Sheffield.

References

[1] Geissen B C, Madhava M, Polk D E and Vander Sande J 1976 *Mater. Sci. Eng.* **23** 145–50
[2] Wang R, Mertz M D, Brimhall J L and Dahlgren S D 1978 *Proc 3rd Int. Conf. on Rapidly Quenched Metals* vol 1 (London: The Metals Society) pp 420–3
[3] Davis S, Fischer M, Geissen B C and Polk D E 1978 *Proc 3rd Int. Conf. on Rapidly Quenched Metals* vol 1 (London: The Metals Society) pp 425–30
[4] Cooper R J 1996 *PhD Thesis* University of Sheffield
[5] Bai Hai Yang, Michaelson C, Gente C and Bormann R 2001 *Phys. Rev.* B **63** 064202
[6] Cooper R J, Randrianantoandro N, Cowlam N and Greneche J-M 1997 *J. Phys.: Condens. Matter* **9** L1–8
[7] Cooper R J, Randrianantoandro N, Cowlam N and Greneche J-M 1997 *Mater. Sci. Eng.* A **226–228** 84
[8] Cooper R J, Randrianantoandro N, Cowlam N and Greneche J-M 2002 at press
[9] Weeber A W and Bakker H 1998 *Physica* B **153** 93–135
[10] Bhatia A B and Thornton D E 1970 *Phys. Rev.* B **2** 3004–12
[11] Li Ji-Chen, Cowlam N and Evetts J E 1993 *J. Non-Cryst. Solids* **156–158** 532–5
[12] Le Caer G and Delcroix P 1996 *Nanostruct. Mater.* **7** 127–35
[13] Le Caer G, Delcroix P, Shen T D and Malaman B 1996 *Phys. Rev.* B **54** 12 775–86
[14] Cocco G, Cowlam N and Enzo S 1994 *Mater. Sci. Eng.* A **178** 29–34